

Response surface methodology for optimization of Phenol photo-catalytic degradation using Carbon-doped TiO₂ nano-photocatalyst

Samira Moghaddam; Mohammad Mahdi Zerafat*; Samad Sabbaghi

Faculty of Advanced Technologies, Nano Chemical Engineering Department, Shiraz University, Shiraz, Iran

Received 08 June 2017; revised 09 October 2017; accepted 23 November 2017; available online 25 November 2017

Abstract

In this research, Carbon-doped TiO₂ nano-photocatalyst is synthesized via sol-gel technique and photo-catalytic degradation of phenol has been studied under ultraviolet and visible light irradiation in a fluidized bed reactor. Various techniques are used to characterize TiO₂ nano-photocatalyst such as X-Ray Diffraction, Fourier transform infrared spectroscopy, Energy Dispersive Spectroscopy and Field Emission Scanning Electron Microscopy. Based on the results, carbon is introduced into titania structure leading to enhanced response towards visible light. Response surface methodology is used to model the effect of various parameters such as pollutant concentration, pH, irradiation time, photo-catalyst content and Carbon to TiO₂ molar ratio. The optimum degradation occurs at pH=9, catalyst content=2.5 (g/L), initial phenol concentration=100 (mg/L), C to TiO₂ molar ratio=2.5 and irradiation time=180 min. The results show that phenol photo-catalytic degradation kinetics follows Langmuir-Hinshelwood model very closely at optimal conditions. Phenol degradation is 75 % under ultraviolet irradiation during a 180 min period and 70 % under visible irradiation during a 420 min period. Based on the results, C-TiO₂ nano-photocatalyst can be a good option for phenol removal under visible light irradiation.

Keywords: Doping; Nano-Photocatalyst; Phenol; Response surface methodology; Ultraviolet.

How to cite this article

Moghaddam S, Zerafat M M, Sabbaghi S. Response surface methodology for optimization of phenol photo-catalytic degradation using Carbon-doped TiO₂ nano-photocatalyst. *Int. J. Nano Dimens.*, 2018; 9 (1): 89-103.

INTRODUCTION

The fast growing world population and reduction of drinking water resources has brought about serious concerns about reliable drinking water supplies throughout the world. Water shortage due to the ever-increasing environmental pollution has made the availability of potable water one of the fundamental problems in today's world and diseases emanated from this pollution threatens the lives of many people. However, water recycling provides access to a viable water resource for a variety of applications [1].

Various pollutants are found in wastewaters such as methylene blue [2], acid green 16 [3], dodecyl benzene sulfonate [4], phenol [5], etc. Phenol and phenolic compounds are among the most serious water contaminants [5], introduced by industrial waste streams such as petrochemical effluents, petroleum refineries and rubber, plastics, adhesive, resin and insecticide manufacturers.

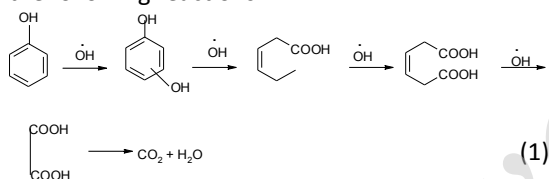
* Corresponding Author Email: mmzerafat@shirazu.ac.ir

These compounds present in industrial effluents can cause genotoxicity in the roots of plants [6]. Although, phenol does not remain in the environment for long, constant release of this compound results in its accumulation in water, air and soil [7]. Phenol is highly toxic even at low concentrations; thus leading to serious damages to the human nervous system. It has also a high affinity to chlorine producing chlorophenol derivatives as compounds more toxic and resilient toward degradation. As a result, phenol removal from industrial effluents using an effective, efficient and affordable method is an essential task [8].

Various methods such as adsorption by activated carbon [9], chemical oxidation [10] and biological treatment [11] have been used to treat phenol or phenol-like compounds, which suffer certain drawbacks like time-consuming and expensive operation and also possible production

of toxic by-products. Therefore, alternatives seem to be vital for the removal of phenol and phenolic compounds [12].

Unique properties of photo-catalytic processes including complete decomposition of pollutant to water and carbon dioxide, simple equipment and high performance in a short period have attracted research attentions recently. Photo-catalytic degradation is started by the absorption of a photon ($h\nu$) with energy equal to or greater than the semiconductor band-gap, electron (e^-) promotion from the valence band (VB) to the conduction band (CB) and formation of a hole (h^+) in the valence band (VB). Holes can react with water and produce hydroxyl radicals with a high redox oxidizing potential. On the other hand, electron conduction band reacts with oxygen and produce O_2^- (Fig.1). O_2^- is also converted to hydroxyl radicals upon subsequent reactions, which are responsible for transformation of toxic pollutants to water and carbon dioxide [13]. Photo-catalytic degradation of phenol (Eq. 1) is widely assumed by the following reactions:



Various nanomaterials and nano-composites are recently introduced as novel photo-catalysts [14]. TiO_2 [15], ZnO [16], WO_3 , ZrO_2 and Fe_2O_3 [17] are used for photo-catalytic degradation of various pollutants [15]. Iqbal *et al.* used ZnO nanoparticles

for degradation of nonyl-phenol ethoxylate under UV and solar irradiation [16]. TiO_2 nanostructures possess properties such as chemical stability, non-toxicity, low cost and high optical activity while suffering certain shortcomings like high speed electron-hole recombination rate and passivity in the wavelength range >400 nm, which is usually overcome by doping of TiO_2 with metals and nonmetals [18]. Table 1 shows a variety of dopants used in other studies in order to enhance the photo-catalytic activity of titania. Based on Table 1 and the results of other research activities on carbon-doped TiO_2 nanoparticles wrapped with nano-graphene [19] and carbon/nitrogen-doped TiO_2 [20] for phenol degradation under visible light, it can be concluded that carbon is considered as a dopant giving high degradation rates in the solar irradiation range which proposes C- TiO_2 nanoparticles as the candidate selected in this study. Doping strategy is performed through various techniques such as hydrolysis [21], hydrothermal [22], oxidation [23] and sol-gel [24]. Sol-gel technique is used in this study due to simple procedure, lack of need for special equipment and viability of various products [25]. Based on our literature review, C- TiO_2 is not used for photo-catalytic removal of phenol from aqueous phase up to now.

Recently, RSM is more extensively used as a statistical tool for modeling and optimization parameters that influence photo-catalytic degradation [39]. RSM is a collection of mathematical and statistical techniques for empirical model building. The objective is to optimize a response

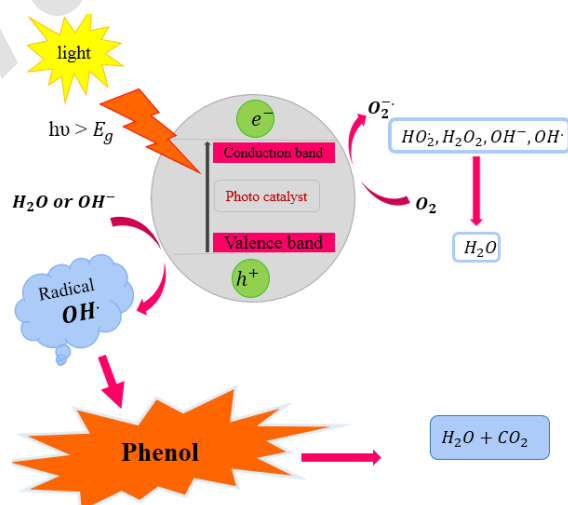


Fig. 1: Mechanism of photo-catalytic degradation.

Table 1: Various dopants and their properties.

Dopant	Technique	Optimal dopant conc. (g/L)	Pollutant	Optimal pollutant conc. (ppm)	Light source	Irradiation time (min)	Efficiency (%)	Ref.
Fe	Hydrolysis	1	Methyl orange	20	UV	360	72	[26]
Pt	Hydrothermal	0.5	Methylene blue	100	UV	60	72	[2]
Pd	Impregnation	1	Acid green 16	122	UV	60	80	[3]
Ag	Photo-reduction	3	Direct Red 23	326	UV	150	55	[27]
C	Sol-gel	1	Methylene blue	10	Solar	127	100	[28]
C/N	-	0.4	Phenol	20	Visible	150	87	[20]
Pr	Sol-gel	1	Phenol	50	UV	120	96.5	[29]
Zr	Sol-gel	2	4-chloro phenol	250	UV	—	—	[30]
Ba	Sol-gel	2	4-chloro phenol	250	UV	—	—	[31]
Sn	Sol-gel/dip coating	12.5	Orange-G	50	UV	60	99.1	[32]
N	Sol gel	0.4	Phenol	20	UV	—	—	[33]
W	Liquid-phase deposition	—	Dodecylbenzene Sulfonate	250	Visible	150	98	[4]
Ce	Co-precipitation	4	Phenol	1000	UV	120	100	[34]
P	Sol-gel	0.2	Rhodamine B	12	Solar	—	85	[35]
Au	Impregnation	1	Acid green 16	122	UV	60	98	[3]
S	Hydrothermal	0.8	Methyl orange	20	UV	70	96	[35-38]

(output variable) influenced by several independent variables (input variables), aimed at the reduction of cost for expensive analysis methods [40].

In this study, C-doped TiO₂ nanoparticles were produced by sol-gel technique and used for photocatalytic degradation of phenol. Furthermore, the impact of effective parameters on phenol removal such as pH, pollutant concentration, catalyst content, C to TiO₂ molar ratio and irradiation time were optimized using RSM investigated under UV and visible light irradiation. Langmuir-Hinshelwood model is also used to calculate the reaction rate constants.

EXPERIMENTAL

Materials

Analytical grades such as titanium tetra isopropoxide (Ti(OPri)₄), ethylene glycol (EG, C₂H₆O₂), citric acid (CA, C₆H₈O₇), ammonia (25%), nitric acid (65-68%) and phenol are supplied by Merck Co. Deionized water was used in the preparation of solutions.

Methods

The apparatus used for characterization of the synthesized nano-photocatalysts and degradation of phenol were X-Ray Diffraction (XRD, Bruker D8 with cupric radiation (Cu K, λ=1.504 Å) emission, 40 kV /40 mA current and 3 scanning rate), Fourier transform infrared spectroscopy (FT-IR,

SHIMADZU 8300 using the standard KBr method), Field Emission Scanning Electron Microscopy (FE-SEM, MIRA 3-XMU, SEM HV=15 kV) and Energy Dispersive Spectroscopy (EDX, MIRA 3-XMU and SEM HV=15 kV).

Experimental Section

- Synthesis of Carbon-doped TiO₂ nanoparticles

In this research, C-TiO₂ nanoparticles are produced by modified sol-gel technique. First, a solution of CA and EG is prepared and Ti (OPri)₄ and nitric acid are added to the initial solution. Finally, ammonia is added to the solution to set pH at a 6-7 value. Molar ratios have been fixed as: [CA/Ti, /CA, CA/EG] = [2:1, 1:3, 1:2]. The sol temperature is set at 90°C, so that gelation is initialized and then baked at 110°C. The Xerogel is formed and the porous grey powder is calcined at 600°C for 2 h in the atmosphere [41]. A schematic of the synthesis procedure is shown in Fig. 2.

- Characterization of C-doped TiO₂ nanoparticles

Properties of the C-doped TiO₂ nanoparticles have been evaluated by various techniques. XRD and EDX analyses are used to determine the size and phase of doped titania, respectively. In order to ensure TiO₂ nanoparticles being doped with carbon, FTIR technique is employed and FE-SEM analysis is also applied to reveal the morphology and structure.

- Photo-catalytic Reactor

The photo-reactor used for the removal of phenol is schematically shown in Fig. 3. This reactor consists of three coaxial tubes. The inner tube is made of quartz and placed at the center of the fluidized bed reactor with an inside UV lamp (8W). The other tubes are made of pyrex. The sample solution is placed between the inner and the middle tubes and the outer tube is used to control the reaction temperature at 30°C. The lamp has a maximum intensity at the light wavelength equal to 254 nm. The solar irradiation experiment was also carried out under xenon light (338 nm).

- Design of Experiments by Response Surface methodology (RSM)

Various parameters such as pH, pollutant concentration, C to TiO₂ molar ratio, catalyst content and irradiation time are assumed to influence phenol degradation. In this research, the variation range for each parameter is considered and various experiments are designed using RSM (Table 2). The relationship between these parameters and the response (dependent parameter) can be described by an empirical second-order polynomial as follows:

$$Y = b_0 + \sum_{i=1}^n b_i x_i + \left(\sum_{i=1}^m b_{ii} x_i \right)^2 + \sum_{i=1}^{n-1} \sum_{j=i+1}^n b_{ij} x_i x_j \quad (2)$$

Where Y, b₀, b_i, b_{ij} and b_{ii} are the predicted

response, constant, linear, interactive and quadratic coefficients, respectively [43]. In addition, x_i and x_j are the coded values for the experimental parameters. The experimental design data were also analyzed using Design-Expert (DX9 MFC Application) software.

- Phenol Removal Experiments

Various concentrations of phenol solution are mixed with nano-photocatalysts (various molar ratios) in the photo-catalytic reactor. In order to determine the optimum value, each test is performed in the 3-11 pH range (adjusted by NaOH (0.2 M) and HCl (0.3 M)). The photo-catalyst is prepared with 3 different molar ratios and degradation of phenol is performed under UV and solar irradiation. Photo-catalysts are centrifuged for 15 min at 5000 rpm and the remaining phenol solution is analyzed using fluorescence spectrometry at 200-700 nm. Absorbance at 299 nm is used to determine phenol concentration. Phenol removal is then given by Eq. (4) as a function of time:

$$C_e = \left[\frac{A_e \times C_0}{A_0} \right] \quad (3)$$

$$\text{Phenol Removal \%} = \left[\frac{C_0 - C_e}{C_0} \right] \quad (4)$$

Where, A₀ and A_e are absorption of phenol at C₀

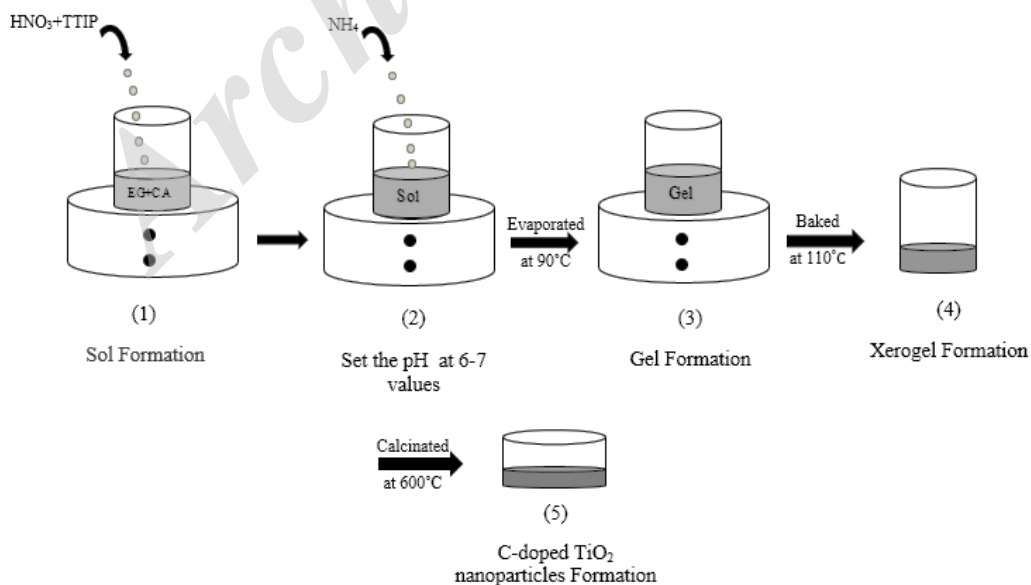


Fig. 2: Schematic of the synthesis procedure for C-doped TiO₂ nanoparticles.

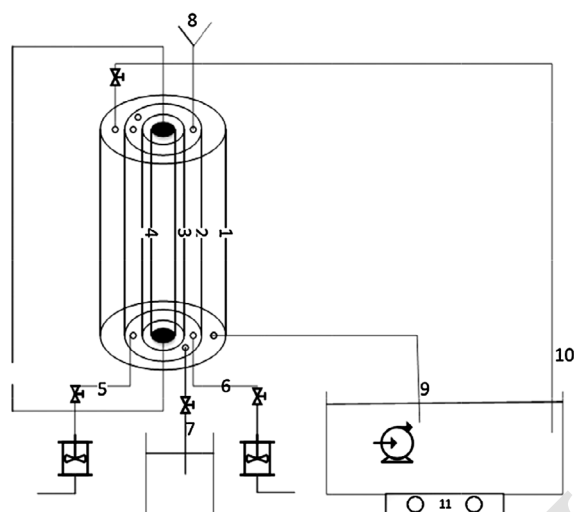


Fig. 3: A schematic of the photo-reactor used for photo-catalytic degradation of phenol: (1) shell, (2) reaction zone, (3) quartz tube, (4) UV lamp, (5 and 6) input air, (7) sample output, (8) sample and catalyst input, (9 and 10) input and output of hot or cold water for temperature control, and (11) heater stirrer.

Table 2: Design of experiments by RSM.

Run	pH	Pollutant conc. (ppm)	Catalyst Content (g/L)	Irradiation time (min)	C to TiO ₂ molar ratio
1	5	60	2	90	2
2	4	20	4	180	2.5
3	9	100	1	180	1.5
4	4	100	1	30	2
5	9	60	1	90	2
6	7	80	4	30	1.5
7	4	100	2	60	1.5
8	4	20	1	180	2
9	7	80	4	30	1.5
10	5	80	3	150	2.5
11	9	20	1	180	2.5
12	4	100	1	180	2.5
13	6	20	1	120	1.5
14	7	100	2	180	2
15	4	60	4	120	2
16	6	20	3	30	2
17	9	20	4	180	2
18	9	100	1	30	2.5
19	9	20	4	30	2.5
20	9	100	4	180	2.5
21	4	100	4	30	2.5
22	5	60	2	90	2
23	4	20	4	30	1.5
24	4	60	1	180	1.5
25	9	60	1	90	2
26	7	40	2	60	2.5
27	7	40	2	60	2.5
28	9	100	4	30	2
29	4	20	1	30	2.5
30	9	20	3	180	1.5
31	4	100	2	60	1.5
32	6	20	4	120	1.5
33	7	60	2	180	1.5
34	4	100	4	180	1.5
35	9	20	1	30	1.5

and C_e as initial and final phenol concentrations in the solution (mg/L).

RESULTS AND DISCUSSION

Characterization of C-TiO₂ nano-photocatalyst

- XRD Analysis

In order to investigate the crystal structure and size and ensure the synthesis of C-doped TiO₂ nanoparticles, X-ray diffraction is used. Fig. 4 shows the diffraction pattern of pure and C-doped TiO₂. Based on Fig. 4, the peak intensity is increased compared with pure Titania, which indicates carbon doping. The size of C-doped TiO₂ nano-crystallites can be obtained using Debye-Scherrer equation:

$$D_{hkl} = k\lambda / \beta \cos\theta \quad (5)$$

Where, D_{hkl} is the mean size of the ordered (crystalline) domains, λ is the X-ray wavelength (1.54×10^{-10}), K is a dimensionless shape factor (with

a typical value of ~ 0.9), β is the line broadening at half the maximum intensity (FWHM) and θ is the Bragg angle. According to equation (5), the crystallite size is estimated to be ~ 28 nm.

- FTIR Analysis

FTIR pattern of pure and C-doped TiO₂ nanoparticles in the range of 200-3700 cm⁻¹ are shown in Fig. 5. The peak at 525.6 cm⁻¹ shows the stretching vibration of Ti-O and the peak at 1423.08 cm⁻¹ is related to hydrocarbon groups. The peak at 2923.08 cm⁻¹ indicates the presence of C-H functional group and the peak at 3438.08 cm⁻¹ indicates the amine group (-OH) [42]. C-doped TiO₂ has an extra peak at 525.6 cm⁻¹ confirming the presence of Ti-O bond in this sample. Also, the peaks of hydrocarbons, functional group of C-H and amines are observed in the pattern of C-doped TiO₂ at a different position compared with pure titania resulting in peak shift.

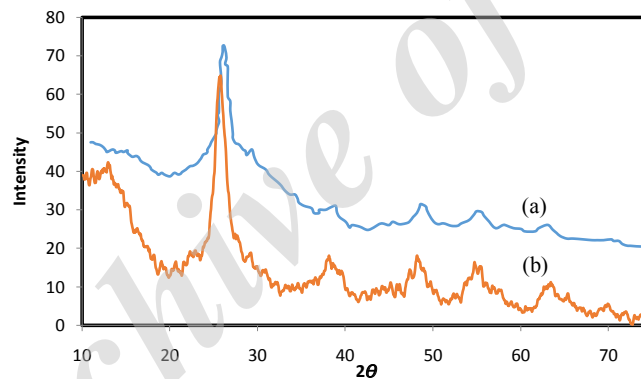


Fig. 4: XRD pattern of a) pure, b) C-doped TiO₂ nanoparticles.

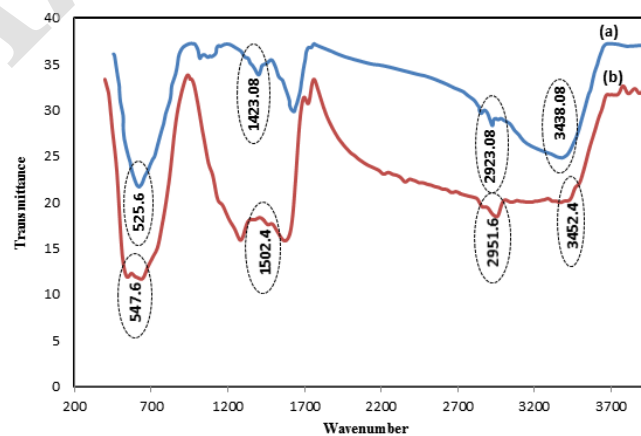


Fig. 5: FTIR pattern of a) pure, b) C-doped TiO₂ nanoparticles.

- FE-SEM Analysis

Figs. 6 (a) & (b) show the FE-SEM micrograph of C-doped TiO₂ nanoparticles with different magnifications. The particle size is estimated as ~ 20 nm with a spherical shape.

- EDX Analysis

EDX analysis is performed in order to identify type and amount of the elements present in the sample (Fig. 7). The intensity of elements such as titanium, carbon and oxygen are 984.9, 202.5 and 240, respectively in the target (Table 3).

- Statistical Analysis

Response surface analysis is used in this study. The relationship between phenol removal as a dependent parameter and independent parameters was obtained using a quadratic fitting method as follows:

$$R = 0.50656 + 1.19657 \times A - 0.046450 \times B + 2.02565 \times C + 0.019653 \times D + 1.90719E-003 \times A \times B - 0.077522 \times A \times C - 2.76254E-003 \times A \times D - 1.85897E-004 \times B \times D + 5.66663E-003 \times C \times D - 0.059700 \times A^2 + 4.46059E-004 \times B^2 - 0.45555 \times C^2 \quad (6)$$

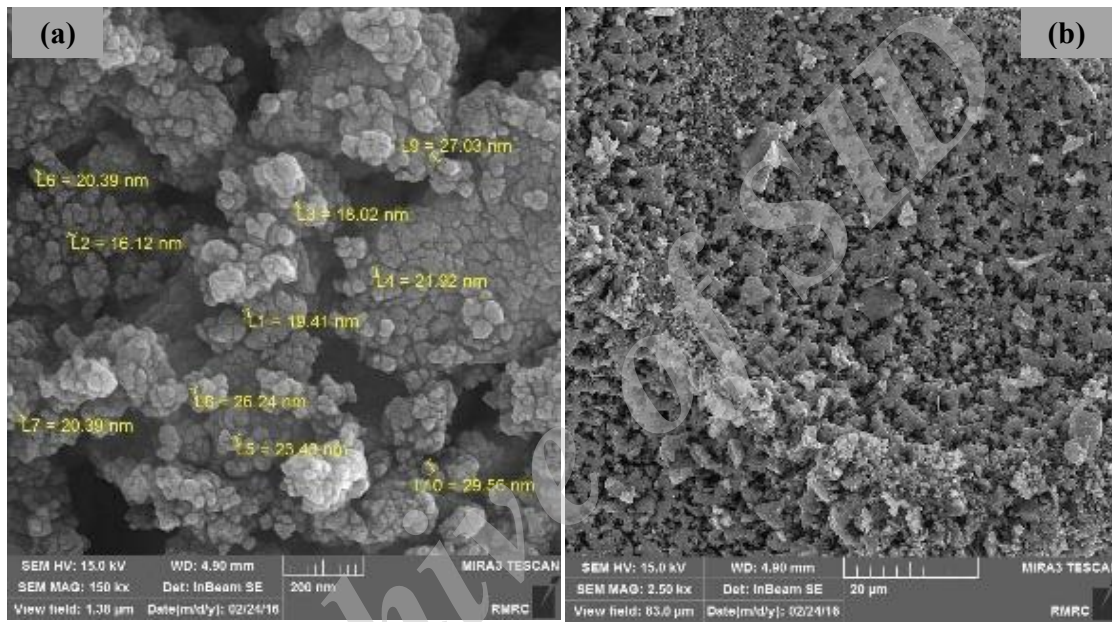


Fig. 6: FE-SEM image of C-doped TiO₂ nanoparticles with a) × 100000 b) × 1500.

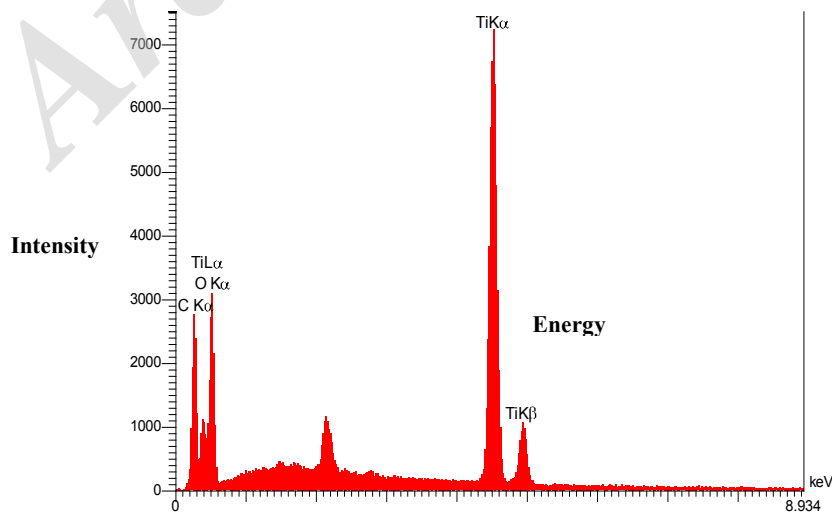


Fig. 7: EDX analysis of C-doped TiO₂ nanoparticles.

Where A, B, C and D are the coded values for process variables pH, phenol concentration (ppm), catalyst content (g/L) and time (min).

According to Table 4, R-squared value of 0.9680 (close to unity) indicates good predictability of the model and Adj. R-Squared for the selected model is equal to 0.9188.

The difference between R-Squared and Adj. R-Squared values is less than 0.2 representing the suitability of data fit. The Pred. R-Squared

obtained is 0.7578 which is acceptable. Herein, the signal to noise ratio estimated by "Adeq. Precision" parameter was equal to 14.829, where ratios > 4 indicate adequate discrimination.

The ANOVA table gives the analysis of variance (ANOVA) for response quadratic model (Table 5). P-values < 0.05 indicate the significance of model terms and values > 0.05 confirm significance. In this study, pH, phenol concentration (ppm), catalyst content (g/L), irradiation time (min) and the interaction of the terms were investigated. The Model F-value of 19.66 and a p-value < 0.0001 implies the model significance. Fig. 8 shows a good agreement between the predicted and actual results.

Effective parameters on photo-catalytic degradation - Solution pH

According to Fig. 9, the rate of removal of phenol is increasing by increasing pH value. Also, the maximum efficiency occurs at pH ≈ 9. The efficiency is very low in the acidic range and enhanced in the alkaline pH range since phenol occurs in the form of phenoxide ions as more reactive compounds leading to stronger interaction with radicals. Another reason is also the high concentration of hydroxide in the alkaline pH range [45]. The rate of removal of phenol is constant at pH > 9

Table 3: EDX elemental microanalysis of C-doped TiO₂ samples.

Samples	wt %
Ti	42.23
C	25.02
O	32.76

Table 4: The values of R given by RSM.

R	Values
R-Squared	0.9680
Adj. R-Squared	0.9188
Pred. R-Squared	0.7578
Adeq. precision	14.829

Table 5: ANOVA for response surface reduced quadratic model- analysis of variance.

Source	Sum of Squares	Df	Mean Square	F Value	p-value Prob > F	
Model	59.78	20	2.99	19.66	< 0.0001	Significant
A-pH	11.86	1	11.86	77.90	< 0.0001	
B-C ₀	0.34	1	0.34	2.23	0.1590	
C-wt%	1.86	1	1.86	12.25	0.0039	
D-time	7.93	1	7.93	52.08	< 0.0001	
E-%doping	0.23	2	0.12	0.77	0.4831	
AB	0.59	1	0.59	3.89	0.0701	
AC	1.56	1	1.56	10.23	0.0070	
AD	4.50	1	4.50	29.53	0.0001	
AE	5.40	2	2.70	17.73	0.0002	
BD	5.96	1	5.96	39.12	< 0.0001	
BE	3.37	2	1.69	11.08	0.0016	
CD	7.13	1	7.13	46.84	< 0.0001	
DE	3.36	2	1.68	11.02	0.0016	
A ²	0.44	1	0.44	2.90	0.1125	
B ²	2.29	1	2.29	15.06	0.0019	
C ²	3.40	1	3.40	22.34	0.0004	
Residual	1.98	13	0.15			
Lack of Fit	1.57	9	0.17	1.73	0.3138	Not significant

because high pH creates favorable conditions for the formation of carbonate ions as good OH⁻ scavengers keeping decomposition rate constant. Also, a large increase in the concentration of hydroxyl ions acts as a barrier against penetration of light into the solution [46].

Figs. 10 (a), (b) & (c), show three dimensional (3-D) response surface plots of removal (%) vs. variables. The influence of pH, phenol concentration (ppm), catalyst content (g/L) and irradiation time (min) on the removal (%) as a response factor are visualized in the 3-D response surface plots.

- Phenol concentration

Effect of phenol concentration on the removal rate is shown in Fig. 11. According to this Fig, the rate of removal of phenol is reducing by increasing phenol concentration. Increased phenol concentration induces competition among hydroxyl oxidizing agents leading to the reduction of removal efficiency [42].

- Catalyst Content

The rate of removal of phenol is increased by increasing the amount of catalyst due to the enhancement of production rate of hydroxyl

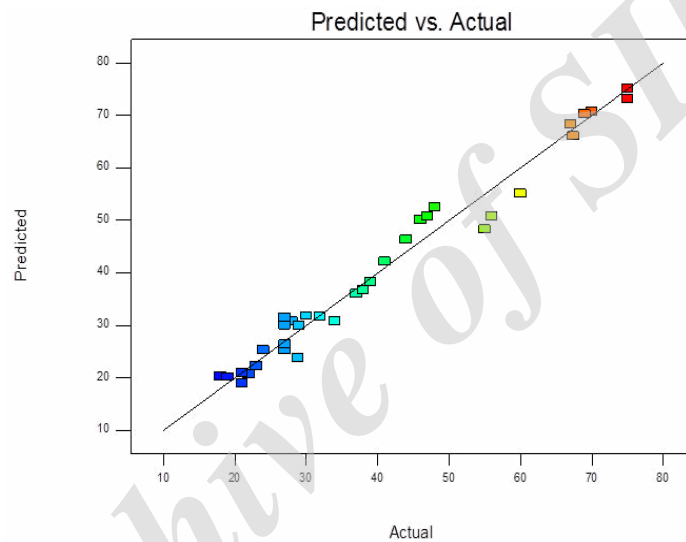


Fig. 8: The plot of predicted vs. phenol removal %.

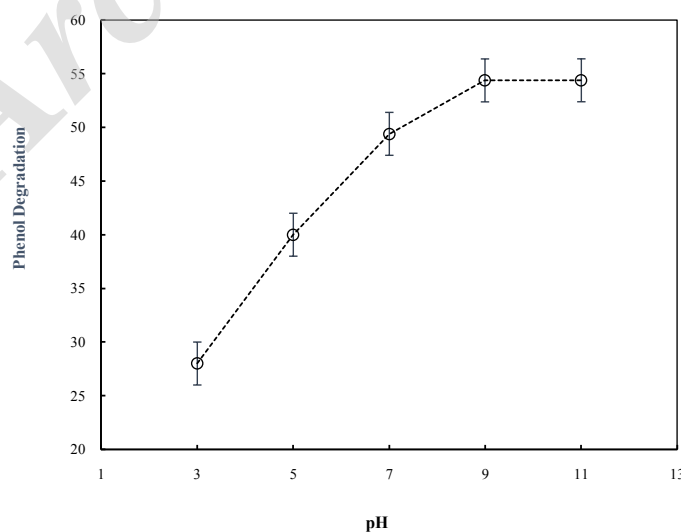


Fig. 9: Influence of pH on the phenol removal rate.

oxidizing agent. Upon reaching a maximum value, further increase in catalyst content leads to the reduction of photo-degradation efficiency because catalyst particles are agglomerated preventing light penetration (Fig. 12) [48]. The highest rate of removal of phenol (50 %) occurs at a catalyst content = 2.5 g/L.

- Irradiation Time

Fig. 13 shows the growth of removal rate by increasing the irradiation time. The reaction rate is decreased by increasing irradiation time due to the enhancement of competition between initial reactants and intermediates over time, which results in reduced reaction of free radicals with nanoparticles [49].

- C to TiO₂ molar ratio

In this research, C-TiO₂ nanoparticles were synthesized with different molar ratios. The results show that different dopant molar ratios have little impact on removal efficiency. All catalysts almost show the same removal rate. Also, increasing or decreasing the carbon content of the composite is ineffective on the removal rate of phenol which suggests lower carbon contents as economical.

Optimization of parameters

A test at optimal conditions was performed under UV and visible light irradiation with conditions shown in Table 6. Fluorescence spectra of UV and visible irradiation are shown in Figs. 14(a & b) and 15(a, b

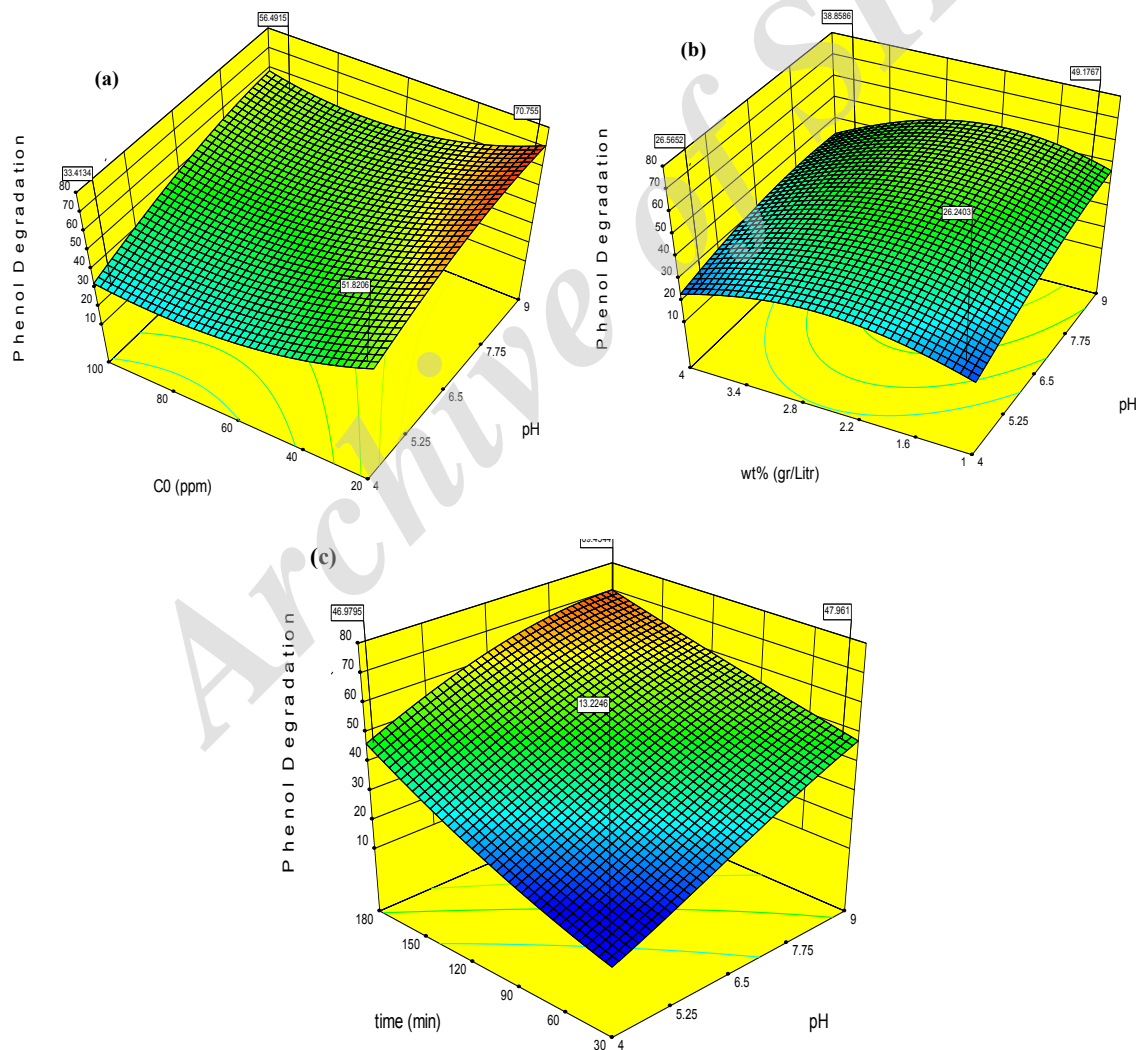


Fig. 10: 3D Response surface graph of the variation of degradation efficiency as a function of a) the pH and phenol concentration (ppm), b) pH and catalyst content (g/L), c) pH and irradiation time (min).

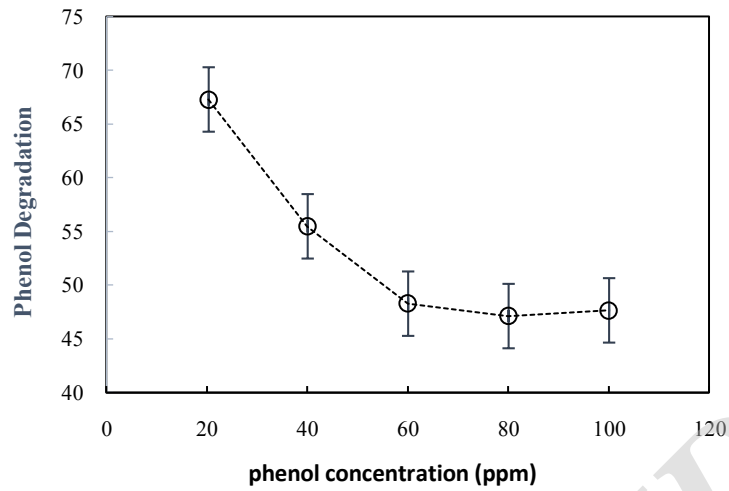


Fig.11. Influence of phenol concentration on the removal rate.

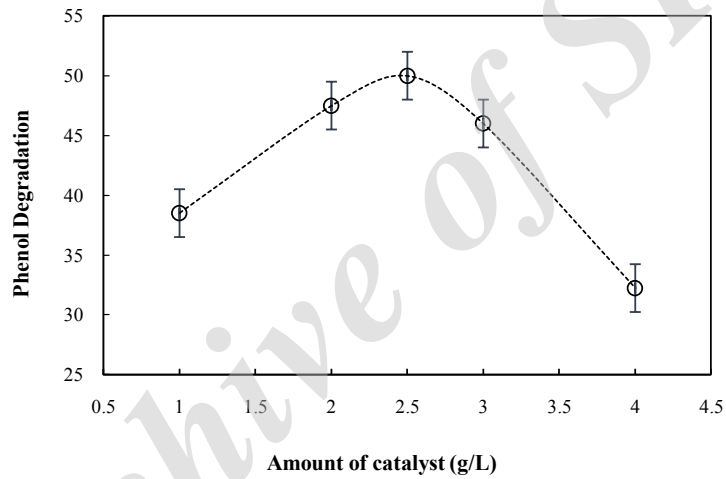


Fig.12. Influence of catalyst content on phenol removal rate.

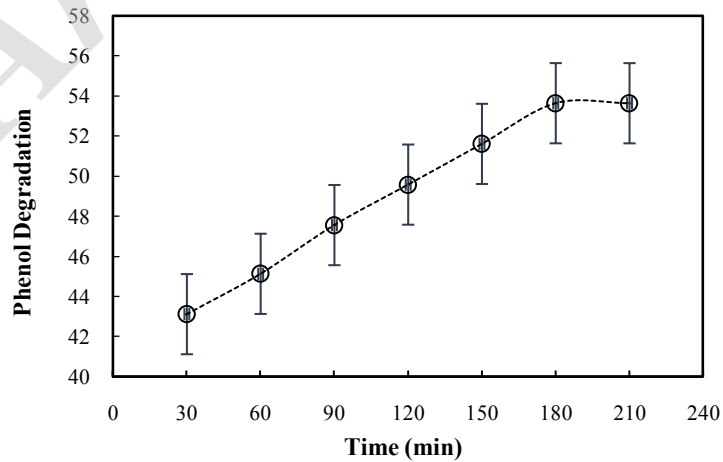


Fig.13. Influence of irradiation time on phenol removal rate.

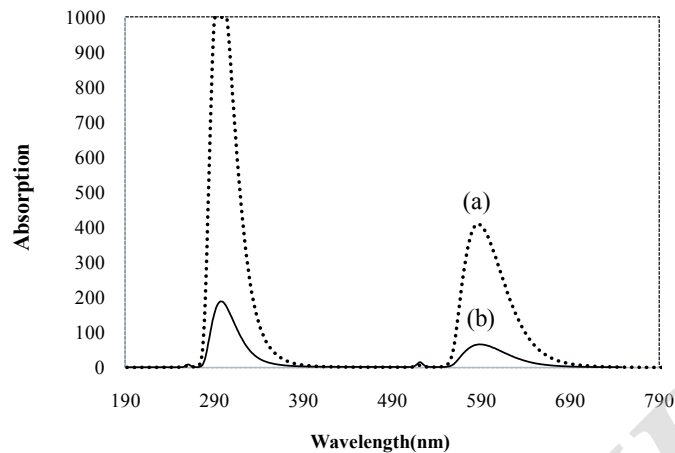


Fig. 14: Fluorescence spectra of phenol 100 ppm a) no irradiation, b) under UV irradiation for 180 min.

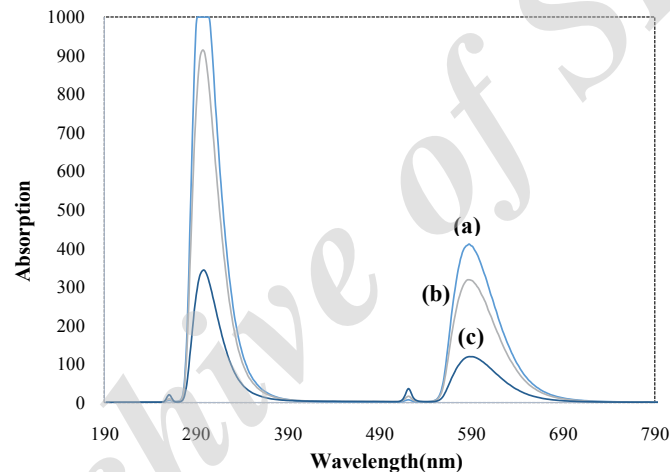


Fig. 15: Fluorescence spectra of phenol 100 ppm a) no irradiation, b) under visible irradiation for 180 min, c) under visible irradiation for 420 min.

& c). Phenol degradation under UV irradiation in a 180 min period is 75% and under visible irradiation in a 180 min period is 30% and 70% in 420 min period. Visible light needs much time to achieve high removal rates of phenol compared to UV due to the lower energy of visible light [18].

Kinetics of phenol degradation

Langmuir-Hinshelwood model is used to determine the kinetics of the photo-catalytic reaction. Langmuir-Hinshelwood model is expressed as follows:

$$r = -\frac{dC}{dt} = \frac{K_r K_{ad} C}{1 + K_{ad} C} \quad (7)$$

Where, r is the photo-catalytic reaction rate

(mg/Lmin), k_r is the reaction rate constant (1/min), C is reactant concentration (mg/L) and K_{ad} the Langmuir adsorption constant (1/min). If the absorbance or concentration of reactants is low, eq. (6) becomes pseudo-first-order and by

Table 6: Optimal conditions.

Effective Parameters	Optimal value
pH	9
Phenol concentration (ppm)	100
Amount of catalyst (g/L)	2.5
C to TiO ₂ molar ratio	2
Irradiation time (min)	180

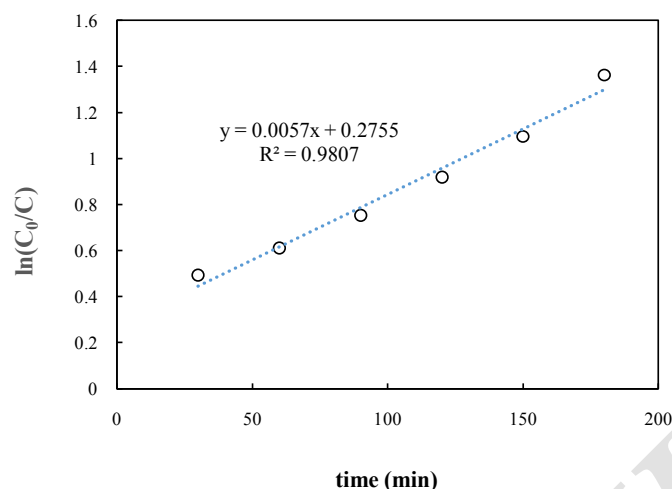


Fig. 16: The kinetics of photo-catalytic degradation of phenol based on Langmuir-Hinshelwood model.

Table 7: Comparison of results of research with the study of other researchers.

Type of the process	Irradiation time (min)	Phenol conc. (ppm)	Phenolic compounds removal efficiency (%)	Researchers
ZnO + Solar light	180	20	40	Peng et al. [51]
CuO/CeO ₂ + UV	240	50	60-70	Paola Massa et al. [52]
TiO ₂ + UV	560	50	83	Rahmani et al. [8]
CuO/ZnO/TiO ₂ + UV	90	50	55	Sadeghi et al. [53]
CN doped TiO ₂ + UV	150	20	87	Abdullah et al. [20]
ZnO + Solar light	1200	50	95	Ashara et al. [16]
γ radiation/H ₂ O ₂	-	100	91	Iqbal et al. [54]
TiO ₂ /H ₂ O ₂ + UV	120	100	92	Muhammad et al. [55]
C-TiO ₂ + UV	180	100	75	This study

integration and taking C_0 as the initial pollutant concentration, eq. (6) is rewritten as follows:

$$\ln\left(\frac{C}{C_0}\right) = -K_r K_{ad} t = -K_{app} t \quad (8)$$

By drawing $-\ln\left(\frac{C}{C_0}\right)$ vs. t , a straight line will be obtained with the slope as the apparent kinetic constant (Fig. 16) [50]. The results showed that the kinetic of phenol photo-catalytic degradation follows Langmuir-Hinshelwood model very closely with $K_{app} = 0.0057$ ($R^2 = 0.9807$).

CONCLUSIONS

In this study, degradation of phenol using C-TiO₂ as a nano-photocatalyst has been studied. Uniform nanoparticles are synthesized through sol-gel technique with spherical shape with an

average ~20 nm size. Photo-catalytic activity of TiO₂ nanoparticles is improved by carbon doping, bringing the photo-catalytic activity in the visible light range. Photo-catalytic degradation of phenol is increased in alkaline environments compared to neutral and acidic conditions, with 75% phenol degradation under UV and 30% under solar irradiation in a 180 min period.

Table 7 shows the results of other studies compared to this study. The results show the efficiency of C-TiO₂ in comparison with other equivalents for phenol removal both from removal point of view and also irradiation period. Based on the results, other dopants can be examined for enhancement of phenol removal or the removal of other more recalcitrant pollutants present in wastewater effluents.

CONFLICT OF INTEREST

The authors declare that there is no conflict of interests regarding the publication of this manuscript.

REFERENCES

- [1] Anderson J., (2003), The environmental benefits of water recycling and reuse. *Water Sci. Tech. Water Supply*. 3: 1-10.
- [2] Li Z., Shen W., He W., Zu X., (2008), Effect of Fe-doped TiO₂ nanoparticle derived from modified hydrothermal process on the photo-catalytic degradation performance on methylene blue. *Hazardous Mater.* 155: 590-594.
- [3] Sakthivel S., Shankar M. V., Palanichamy M., Arabindoo B., Bahnemann D. W., Murugesan V., (2004), Enhancement of photo-catalytic activity by metal deposition: Characterization and photonic efficiency of Pt, Au and Pd deposited on TiO₂ catalyst. *Water Res.* 38: 3001-3008.
- [4] Devi L. G., Rajashekhar K. E., (2011), A kinetic model based on non-linear regression analysis is proposed for the degradation of phenol under UV/solar light using nitrogen doped TiO₂. *Molec. Catal. A: Chem.* 334: 65-76.
- [5] Akbal F., Onar A. N., (2003), Photo-catalytic degradation of phenol. *Environ. Monitor. Asses.* 83: 295-302.
- [6] Iqbal M., (2016), Vicia faba bioassay for environmental toxicity monitoring: A review. *Chemosphere.* 144: 785-802.
- [7] Ksibi M., Zemzemi A., Boukchina R., (2003), Photo-catalytic degradability of substituted phenols over UV irradiated TiO₂. *Photochem. Photobiol. A: Chem.* 159: 61-70.
- [8] Wang K. H., Hsieh Y. H., Chou M. Y., Chang C. Y., (1999), Photocatalytic degradation of 2-chloro and 2-nitrophenol by titanium dioxide suspensions in aqueous solution. *Appl. Catal. B: Environ.* 21: 1-8.
- [9] Brasquet C., Le Cloirec P., (1997), Adsorption onto activated carbon fibers: Application to water and air treatments. *Carbon.* 35: 1307-1313.
- [10] Huang C. P., Dong C., Tang Z., (1993), Advanced chemical oxidation: Its present role and potential future in hazardous waste treatment. *Waste Manag.* 13: 361-377.
- [11] Lawrence A. W., McCarty P. L., (1970), Unified basis for biological treatment design and operation. *Sanitary Eng. Division.* 96: 757-778.
- [12] Kurniawan T. A., Chan G. Y., Lo W. H., Babel S., (1006), Physico-chemical treatment techniques for wastewater laden with heavy metals. *Chem. Eng. J.* 118: 83-98.
- [13] Chong M. N., Jin B., Chow C. W., Saint C., (2010), Recent developments in photo-catalytic water treatment technology: A review. *Water Res.* 44: 2997-3027.
- [14] Shanmugapriya S., Premalatha M., Anantharaman N., (2008), Solar photo-catalytic treatment of phenolic wastewater potential, challenges and opportunities. *Eng. Appl. Sci.* 3: 36-41.
- [15] Rahmani A., Enayati M. A., (2006), Investigation of photo-catalytic degradation of phenol through UV/TiO₂ Process. *Water Wastewater.* 17: 32-37.
- [16] Ashar A., Iqbal M., Bhatti I. A., Ahmad M. Z., Qureshi K., Nisar J., Bukhari I. H., (2016), Synthesis, characterization and photocatalytic activity of ZnO flower and pseudo-sphere: Nonylphenol ethoxylate degradation under UV and solar irradiation. *J. Alloys and Comp.* 678: 126-136.
- [17] Byrne J. A., Fernandez-Ibanez P. A., Dunlop P. S., Alrousan D., Hamilton J. W., (2011), Photocatalytic enhancement for solar disinfection of water: A review. *Int. J. Photoenergy.* 2011: Article ID 798051, 12 pages.
- [18] Zhou M., Yu J., Cheng B., (2006), Effects of Fe-doping on the photo-catalytic activity of mesoporous TiO₂ powders prepared by an ultrasonic method. *Hazard. Mater.* 137: 1838-1847.
- [19] Yu S., Yun H. J., Kim Y. H., Yi J., (2014), Carbon-doped TiO₂ nanoparticles wrapped with nanographene as a high performance photocatalyst for phenol degradation under visible light irradiation. *Appl. Catal. B: Environmen.* 144: 893-899.
- [20] Abdullah A. M., Al-Thani N. J., Tawbi K., Al-Kandari H., (2016), Carbon/nitrogen-doped TiO₂: New synthesis route, characterization and application for phenol degradation. *Arab. J. Chem.* 9: 229-237.
- [21] Sun Y., Cheng J., (2002), Hydrolysis of lingo-cellulosic materials for ethanol production: A review. *Bioresource Technol.* 83: 1-11.
- [22] Zhu J., Zheng W., He B., Zhang J., Anpo M., (2004), Characterization of Fe-TiO₂ photo-catalysts synthesized by hydrothermal method and their photo-catalytic reactivity for photo degradation of XRG dye diluted in water. *Molecul. Catal. A: Chem.* 216: 35-43.
- [23] Andreozzi R., Caprio V., Insola A., Marotta R., (1999), Advanced oxidation processes (AOP) for water purification and recovery. *Catalysis Today.* 53: 51-59.
- [24] Rahman I. A., Padavettan V., (2012), Synthesis of silica nanoparticles by sol-gel: Size-dependent properties, surface modification and applications in silica-polymer nanocomposites: A review. *Nanomaterials.* 8: 1-8.
- [25] Hench L. L., West J. K., (1990), The sol-gel process. *Chem. Rev.* 90 (1): 33-72.
- [26] Tong T., Zhang J., Tian B., Chen F., He D., (2008), Preparation of Fe₃-doped TiO₂ catalysts by controlled hydrolysis of titanium alkoxide and study on their photo-catalytic activity for methyl orange degradation. *J. Hazard. Mater.* 155: 572-579.
- [27] Sobana N., Selvam K., Swaminathan M., (2008), Optimization of photo-catalytic degradation conditions of Direct Red 23 using nano-Ag doped TiO₂. *Sep. Purifi. Tech.* 62: 648-653.
- [28] Xiao Q., Zhang J., Xiao C., Si Z., Tan X., (2008), Solar photo-catalytic degradation of methylene blue in carbon-doped TiO₂ nanoparticles suspension. *Solar Energy.* 82: 706-713.
- [29] Chiou C. H., Juang R. S., (2007), Photo-catalytic degradation of phenol in aqueous solutions by Pr-doped TiO₂ nanoparticles. *J. Hazard. Mater.* 149: 1-7.
- [30] Venkatachalam N., Palanichamy M., Arabindoo B., Murugesan V., (2007), Enhanced photo-catalytic degradation of 4-chlorophenol by Zr⁴⁺ doped nano TiO₂. *Molec. Catal. A: Chem.* 266: 158-165.
- [31] Venkatachalam N., Palanichamy M., Murugesan V., (2007), Sol-gel preparation and characterization of alkaline earth metal doped nano TiO₂: Efficient photo-catalytic degradation of 4-chlorophenol. *Molec. Catal. A.* 273: 177-185.
- [32] Sun J., Wang X., Sun J., Sun R., Sun S., Qiao L., (2006), Photo-catalytic degradation and kinetics of Orange G using nano-sized Sn (IV)/TiO₂/AC photo-catalys. *Molec. Catal. A: Chem.* 260: 241-246.
- [33] Devi L. G., Rajashekhar K. E., (2011), A kinetic model based on non-linear regression analysis is proposed for the degradation of phenol under UV/solar light using nitrogen

- doped TiO₂ *Molec. Catal A: Chem.* 334: 65-76.
- [34] Yang S., Zhu W., Wang J., Chen Z., (2008), Catalytic wet air oxidation of phenol over CeO₂-TiO₂ catalyst in the batch reactor and the packed-bed reactor. *Hazard. Mater.* 153: 1248-1253.
- [35] Lv Y., Yu L., Huang H., Liu H., Feng Y., (2009), Preparation, characterization of P-doped TiO₂ nanoparticles and their excellent photo-catalytic properties under the solar light irradiation. *Alloys & Comp.* 488: 314-319.
- [36] Mori K., Maki K., Kawasaki S., Yuan S., Yamashita H., (2008), Hydrothermal synthesis of TiO₂ photo-catalysts in the presence of NH₄F and their application for degradation of organic compounds. *Chem. Eng. Sci.* 63: 5066-5070.
- [37] Janitabar Darzi S., Mahjoub A. R., Bayat A., (2016), Synthesis and characterization of visible light active S-doped TiO₂ nano-photocatalyst. *Int. J. Nano Dimens.* 7: 33-40.
- [38] Zakeri S. M. E., Asghari M., Feilizadeh M., Vosoughi M., (2014), A visible light driven doped TiO₂ nano-photocatalyst: Preparation and characterization. *Int. J. Nano Dimens.* 5: 329-335.
- [39] Liu H. L., Chiou Y. R., (2005), Optimal de-colorization efficiency of Reactive Red 239 by UV/TiO₂ photo-catalytic process coupled with response surface methodology. *Chem. Eng. J.* 112: 173-179.
- [40] Box G. E., Draper N. R., (1987), Empirical model-building and response surfaces (Vol. 424). New York: Wiley.
- [41] Xiao Q., Zhang J., Xiao C., Si Z., Tan X., (2008), Solar photo-catalytic degradation of methylene blue in carbon-doped TiO₂ nanoparticles suspension. *Solar Energy.* 82: 706-713.
- [42] Mohammadi M., Sabbaghi S., (2014), Photo-catalytic degradation of 2, 4-DCP wastewater using MWCNT/TiO₂ nano-composite activated by UV and solar light. *Environ. Nanotech. Monitoring Manag.* 1-2: 24-29.
- [43] Rasouli F., Aber S., Salari D., Khataee A. R., (2014), Optimized removal of Reactive Navy Blue SP-BR by organo-montmorillonite based adsorbent through central composite design. *Appl. Clay Sci.* 87: 228-34.
- [44] Pavia D. L., Lampman G. M., Kriz G. S., Vyvyan J. A. (4th Ed.), (2008), Introduction to Spectroscopy, Gengage Learning.
- [45] Vinu R., Madras G., (2011), Photo-catalytic degradation of water pollutants using nano-TiO₂, In Energy efficiency and renewable energy through nanotechnology. *Energy Efficiency and Renewable Energy through Nanotech.* Springer. 625-677.
- [46] Bubacz K., Choina J., Dolat D., Morawski A. W., (2010), Methylene blue and phenol photo-catalytic degradation on nanoparticles of anatase TiO₂. *Environm. Studies.* 19: 672-685.
- [47] Chiou C. H., Wu C. Y., Juang R. S., (2008), Influence of operating parameters on photo-catalytic degradation of phenol in UV/TiO₂ process. *Chem. Eng.* 139: 322-329.
- [48] Liou R. M., Chen S. H., Hung M. Y., Hsu C. S., Lai J. Y., (2005), Fe (III) supported on resin as effective catalyst for the heterogeneous oxidation of phenol in aqueous solution. *Chemosphere.* 59: 117-125.
- [49] Hayat K., Gondal M. A., Khaled M. M., Ahmed S., Shemsi A. M., (2011), Nano ZnO synthesis by modified sol gel method and its application in heterogeneous photo-catalytic removal of phenol from water. *Appl. Catal A: General.* 393: 122-129.
- [50] Chong M. N., Jin B., Chow C. W., Saint C., (2010), Recent developments in photo-catalytic water treatment technology: A review. *Water Research.* 44: 2997-3027.
- [51] Barakat M. A., Schaeffer H., Hayes G., Ismat-Shah S., (2005), Photo-catalytic degradation of 2-chlorophenol by Co-doped TiO₂ nanoparticles. *Appl. Catal. B: Environ.* 57: 23-30.
- [52] Massa P., Ivorra F., Haure P., Fenoglio R., (2011), Catalytic wet peroxide oxidation of phenol solutions over CuO/CeO₂ systems. *Hazard. Mater.* 190: 1068-1073.
- [53] Mohammadi M., Sabbaghi S., Sadeghi H., Zerafat M. M., Pooladi R., (2016), Preparation and characterization of TiO₂/ZnO/CuO nanocomposite and application for phenol removal from wastewaters. *Desalination & Water Treatment.* 57: 799-809.
- [54] Iqbal M., Bhatti I. A., (2015), Gamma radiation/H₂ O₂ treatment of a nonylphenol ethoxylates: Degradation, cytotoxicity, and mutagenicity evaluation. *J. Hazard. Mater.* 299: 351-360.
- [55] Ahamd M. Z., Ehtisham-ul-Haque S., Nisar N., Qureshi K., Ghaffar A., Abbas M., Iqbal, M., (2017), Detoxification of photo-catalytically treated 2-chlorophenol: Optimization through response surface methodology. *Water Sci. Technol.* wst 2017152.